Angewandte Chemie
Eine Zeitschrift der Gesellschaft Deutscher Chemiker

Supporting Information

69451 Weinheim, Germany

Reversible Three-State Switching of Multicolor Fluorescence Emission by Multiple Stimuli Modulated FRET Processes within Thermoresponsive Polymeric Micelles**

Changhua Li, Yanxi Zhang, Jinming Hu, Jianjun Cheng, and Shiyong Liu**

anie_201002203_sm_miscellaneous_information.pdf

Experimental Section

Materials. *N*-Isopropylacrylamide (NIPAM, 97%, Tokyo Kasei Kagyo Co.) was purified by recrystallization from a mixture of benzene and *n*-hexane (1/3, v/v). Styrene (St, 99.5%, Beijing Chemical Factory) was successively washed with aqueous NaOH (5.0 wt %) and water, then distilled over CaH_2 at reduced pressure. 4-Chloro-7-nitrobenzofurazan (NBD-Cl, 99%), 2,3,3-trimethylindolenine (98%), and 5-nitrosalicylaldehyde (98%) were purchased from Alfa and used as received. 2,2-Azoisobutyronitrile (AIBN) was recrystallized from 95% ethanol. Rhodamine B (RhB, Acros), hydrazine hydrate, and all other reagents (Sinopharm Chemical Reagent Co.) were used as received. Acryloyl chloride (Sinopharm Chemical Reagent Co.) was distilled prior to use. Dichloromethane (CH_2Cl_2) and acetonitrile (MeCN) were dried over CaH_2 and distilled just prior to use. Water was deionized with a Milli-Q SP reagent water system (Millipore) to a specific resistivity of 18.4 MΩcm. S-1-propyl-S'-(α,α'-dimethyl-α''-acetic acid)trithiocarbonate (PDMAT),[1] 4-(2-Acryloyloxyethylamino)-7-

nitro-2,1,3-benzoxa-diazole (NBDAE),[2] 10-(2-methacryloxyethyl)-30,30-dimethyl-6-nitro-spiro(2H-1-benzo-pyran-2,20-indoline) (SPMA),[3] and rhodamine B hydrazide[4] were synthesized according to literature procedures.

Sample Synthesis. Synthetic routes employed for the synthesis of rhodamine B-based monomer, RhBAM, and P(St-*co*-NBDAE-*co*-SPMA)$_{20}$-*b*-P(NIPAM-*co*-RhBAM)$_{60}$ are shown in Schemes S1and S2, respectively.

Synthesis of RhBAM Monomer (Scheme S1). Rhodamine B hydrazide (0.50 g, 1.1 mmol) was dissolved in 20 mL dry MeCN, followed by the dropwise addition of acryloyl chloride (2.98 g, 33.0 mmol). The reaction mixture was refluxed for 15 min. The precipitates were collected by filtration and washed with dry MeCN for three times. The crude product was dissolved in CH_2Cl_2 and washed with saturated $NaHCO_3$ aqueous solution for three times. The organic phase was then dried over anhydrous Na_2SO_4 and filtrated. After removing all the solvents, the product was obtained as a violet solid (0.21 g, yield: 37.6%). ^{1}H NMR ($CDCl_3$, δ, ppm, TMS; Figure S1): 7.94 (1H, Ar*H*), 7.64-7.37 (2H, Ar*H*), 7.07 (1H, Ar*H*), 6.65 (2H, xanthene-*H*), 6.45-6.13 (4H, xanthene-*H*), 5.93(1H, -CH=CH*H*), 5.58 (1H, -C*H*=CHH), 5.31 (1H, -CH=C*H*H), 3.31 (8H, -NCH_2CH$_3$), 1.14 (12H, -NCH$_2$CH_3).

Synthesis of P(St-co-NBDAE-co-SPMA) (Scheme S2). Typical procedures employed for the synthesis of NBDAE and SPMA labeled PS precursor, P(St-*co*-NBDAE-*co*-SPMA)$_{20}$, are as follows. A reaction tube was charged with St (2.0 g, 19.2 mmol), NBDAE (2.8 mg, 9.6 μmol), SPMA (40.4 mg, 96 μmol), PDMAT (28.6 mg, 0.12 mmol), AIBN (2.0 mg, 12 μmol), and 1,4-dioxane (2.0 g). The mixture was degassed by three freeze-pump-thaw cycles and then sealed under vacuum. The polymerization was conducted at 80 ^{o}C for 12 h. The viscous mixture was diluted with CH_2Cl_2 and then precipitated into an excess of methanol for three times. After drying in a vacuum oven overnight at room temperature, P(St-*co*-NBDAE-*co*-SPMA)$_{20}$ was obtained as a yellowish powder (0.38 g, yield: 19%; $M_{n,GPC}$ = 2.1 kDa, M_w/M_n = 1.08).

Synthesis of P(St-co-NBDAE-co-SPMA)-b-P(NIPAM-co-RhBAM) Diblock Copolymer (Scheme S2). Typical procedures employed for the RAFT synthesis of P(St-*co*-NBDAE-*co*-SPMA)$_{20}$-*b*-P(NIPAM-*co*-RhBAM)$_{60}$ diblock copolymer are as follows. Into a reaction tube equipped with a magnetic stirring bar, NIPAM (0.75 g, 6.64 mmol), RhBAM (12.3 mg, 24

μmol), P(St-*co*-NBDAE-*co*-SPMA)$_{20}$ (0.20 g, 83 μmol), AIBN (1.6 mg, 10 μmol), and 1,4-dioxane (1.0 mL) were charged. The tube was carefully degassed by three freeze-pump-thaw cycles and then sealed under vacuum. After stirring at 70 ^{o}C for 5 h, the reaction tube was quenched into liquid nitrogen, opened, and diluted with 1,4-dioxane; the mixture was then precipitated into an excess of cold diethyl ether to yield a pink powder. The obtained diblock copolymer was then dissolved in THF, and AIBN (20 equiv relative to diblock copolymer) was added to the solution. After purging the solution with N_2, the mixture was stirred at 70 ^{o}C for 2 h. The diblock copolymer was isolated by repeated precipitation from THF into cold diethyl ether for three times. After drying in a vacuum oven overnight at room temperature, P(St-*co*-NBDAE-*co*-SPMA)$_{20}$-*b*-P(NIPAM-*co*-RhBAM)$_{60}$ was obtained as a slightly pink powder (0.66 g, yield: 69%; $M_{n,GPC}$ = 7.9 kDa, M_w/M_n = 1.14). The molar contents of NBDAE and SPMA moieties (relative to PS block), and RhBAM moieties (relative to PNIPAM block) were determined to be ~0.1, ~0.8, and ~0.3 mol%, respectively, based on UV absorbance calibration curves.

Instruments. *Nuclear Magnetic Resonance (NMR) Spectroscopy.* All ^{1}H NMR spectra were recorded on a Bruker AV300 NMR spectrometer (resonance frequency of 300 MHz for ^{1}H NMR) operated in the Fourier transform mode.

Gel Permeation Chromatography (GPC). Molecular weights and molecular weight distributions were determined by gel permeation chromatography (GPC) with Waters 1515 pump and Waters 2414 differential refractive index detector (set at 30 ^{o}C). It used a series of two linear Styragel columns (HT2 and HT4) at an oven temperature of 45 ^{o}C. The eluent was THF at a flow rate of 1.0 mL/min. A series of low polydispersity polystyrene standards were employed for the GPC calibration.

*Laser Light Scattering (LLS)***.** A commercial spectrometer (ALV/DLS/SLS-5022F) equipped with a multi-tau digital time correlator (ALV5000) and a cylindrical 22 mW UNIPHASE He-Ne laser (λ_0 = 632 nm) as the light source was employed for dynamic laser light scattering (LLS) measurements. Scattered light was collected at a fixed angle of 90° for duration of ~10 min. Distribution averages and particle size distributions were computed using cumulants analysis and CONTIN routines. All data were averaged over three measurements.

Surface Tensiometry. Equilibrium surface tensions were measured using a JK99B

tensiometer with a platinum plate. The measuring accuracy of the device as reported by the manufacturer is ± 0.1 mN/m. The reported surface tension was the average of four to five measurements that were taken after allowing each of the solutions to equilibrate in the instrument at a temperature of 25.0 ± 0.2 °C.

Fluorescence Measurements. Fluorescence spectra were recorded using a RF-5301/PC (Shimadzu) spectrofluorometer. The temperature of the water-jacketed cell holder was controlled by a programmable circulation bath. The slit widths were set at 5 nm for both excitation and emission.

UV-Vis Spectroscopy. All UV-Vis spectra were acquired on a Unico UV/Vis 2802PCS spectrophotometer. A thermostatically controlled couvette was employed and the heating rate was 0.2 ^{o}C min^{-1}.

Atomic Force Microscopy (AFM). AFM measurements were performed on a Digital Instrument Multimode Nanoscope IIID operating in the tapping mode under ambient conditions. Silicon cantilever (RFESP) with resonance frequency of ~80 kHz and spring constant of ~3 N/m was used. The set-point amplitude ratio was maintained at 0.7 to minimize sample deformation induced by the tip. The samples were prepared by dip coating 0.05 g/L aqueous micellar solutions onto freshly cleaved mica surfaces.

Discussion. *Calculation of FRET Efficiency under Varying External Stimuli.* To estimate the FRET efficiency (E), we employed a simplified equation, $E = 1-I/I_0$, where I_0 and I are the NBDAE donor fluorescence intensity at 518 nm before and after external stimuli (e.g. pH and UV) was actuated, respectively. The experimental E of NBDAE/RhBAM FRET pair is 37.2% at 25 ^{o}C and pH 3, which increases to 83.3% at 35 ^{o}C and pH 3. For NBDAE/SPMA FRET pair, the experimental E is 95.4% at pH 7 upon UV irradiation for 2 min.

pH-Dependence of CMC and Micellar Sizes. Diblock copolymer micelles consist of hydrophobic PS cores and hydrophilic PNIPAM coronas covalently attached with RhBAM dyes. Although RhBAM are pH-sensitive, their labeling content is quite low (0.3 mol% relative to NIPAM repeating units), thus on average there exists only 1 RhBAM dye for ~5.6 diblock copolymer chains. Preliminary experiments revealed that both CMC and micellar size are independent of solution pH in the range of pH 3-9.

References

[1] J. T. Lai, D. Filla, R. Shea, *Macromolecules* 2002, *35*, 6754-6756.

[2] S. Uchiyama, Y. Matsumura, A. P. de Silva, K. Iwai, *Anal. Chem.* 2003, *75*, 5926-5935.

[3] F. M. Raymo, S. Giordani, *J. Am. Chem. Soc.* 2001, *123*, 4651-4652.

[4] X. F. Yang, X. Q. Guo, Y. B. Zhao, *Talanta* 2002, *57*, 883-890.

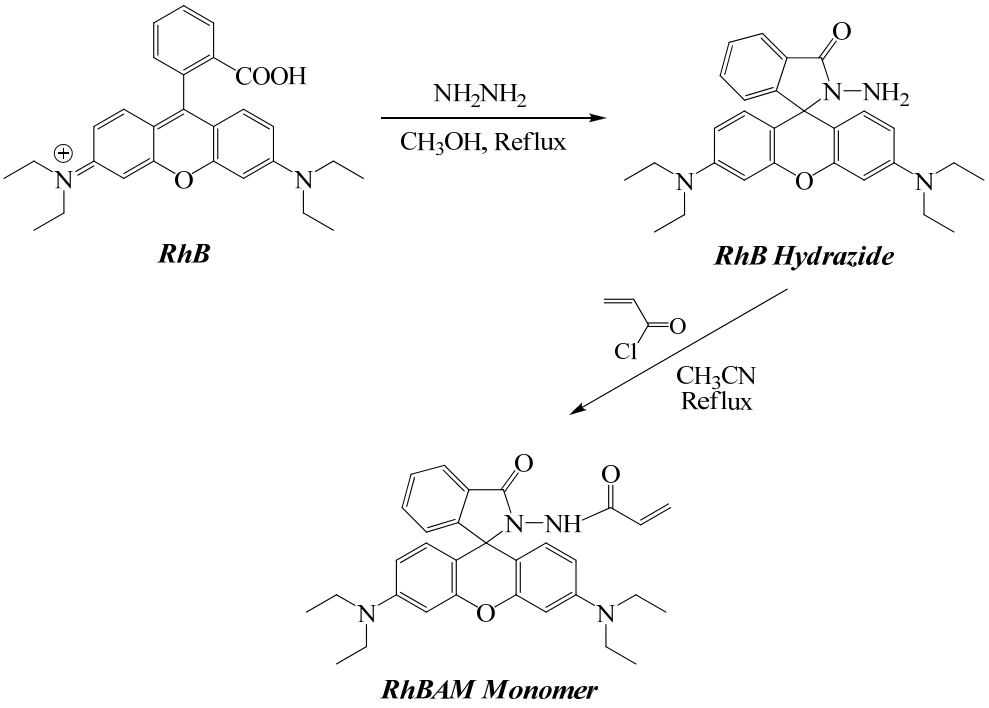

Scheme S1. Synthetic schemes employed for the synthesis of rhodamine B-based monomer (RhBAM), which exhibits pH-switchable on/off fluorescence emission.

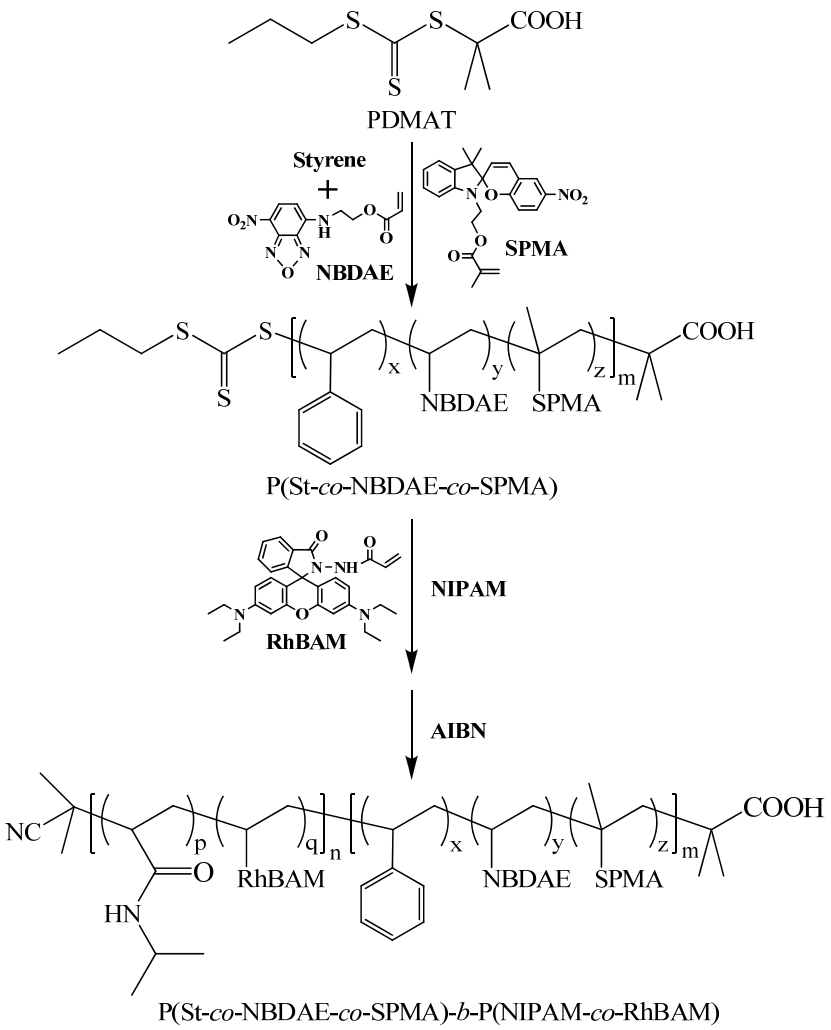

Scheme S2. Synthetic schemes employed for the RAFT synthesis of well-defined amphiphilic and thermoresponsive diblock copolymer, P(St-*co*-NBDAE-*co*-SPMA)$_{20}$-*b*-P(NIPAM-*co*-RhBAM)$_{60}$, bearing NBDAE and photo-switchable SPMA moieties in the hydrophobic PS block, and pH-switchable RhBAM dyes in the thermoresponsive PNIPAM block.

Table S1. Molecular Parameters of Amphiphilic and Thermoresponsive Diblock Copolymer Synthesized in this Work.

Samples	DP_{NMR} [a]		M_n [b] (kDa)	PDI [b]	CMC [c] (mg/L)	D_h [d] (nm)
	PS block	PNIPAM block				
P(St-*co*-NBDAE)$_{20}$-*b*-PNIPAM$_{61}$	20	61	8.0	1.12	2.3	48
PS$_{21}$-*b*-P(NIPAM-*co*-RhBAM)$_{60}$	21	60	7.9	1.12	2.1	49
P(St-*co*-SPMA)$_{21}$-*b*-PNIPAM$_{60}$	21	60	7.9	1.12	2.1	50
P(St-*co*-NBDAE)$_{20}$-*b*-P(NIPAM-*co*-RhBAM)$_{60}$	20	60	7.9	1.13	2.3	49
P(St-*co*-NBDAE-*co*-SPMA)$_{20}$-*b*-PNIPAM$_{60}$	20	60	7.8	1.12	2.3	48
P(St-*co*-NBDAE-*co*-SPMA)$_{20}$-*b*-P(NIPAM-*co*-RhBAM)$_{60}$	20	60	7.9	1.14	2.3	49

[a] Determined by ^{1}H NMR analysis in $CDCl_3$. [b] Obtained from GPC analysis using THF as eluent. [c] Determined by surface tensiometry at 25 ^oC. [d] Determined by DLS at 25 ^oC, scattered light was collected at a fixed angle of 90° for duration of ~10 min.

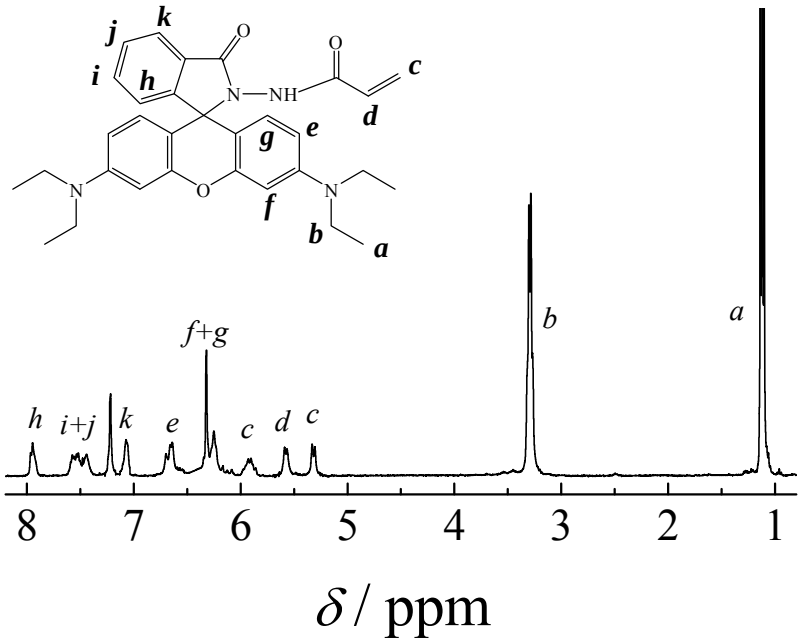

Figure S1. ^{1}H NMR spectrum recorded in $CDCl_3$ for rhodamine B-based monomer, RhBAM.

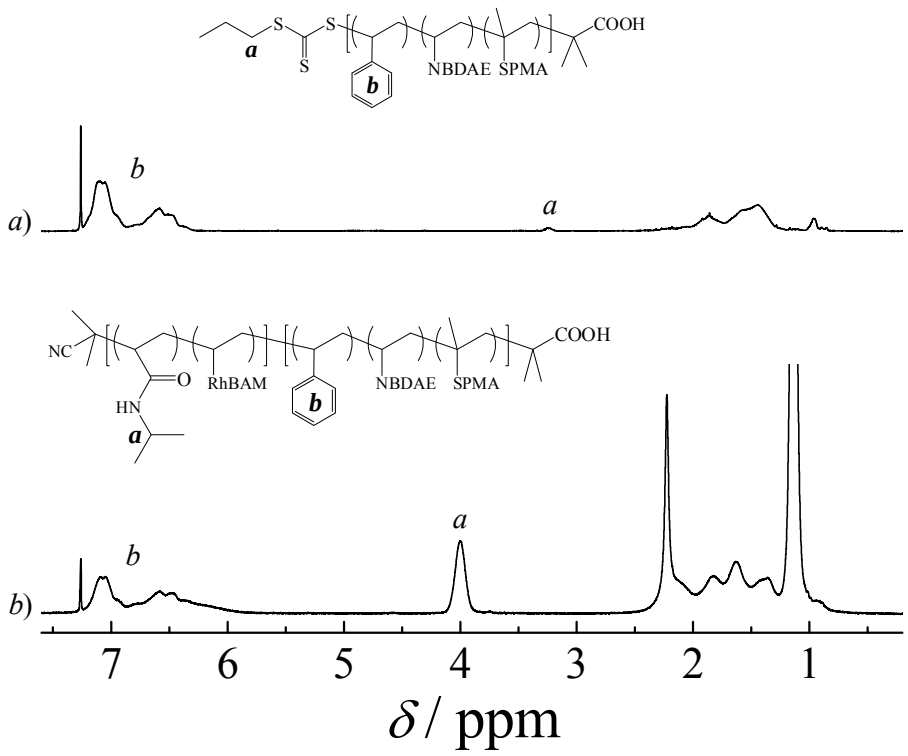

Figure S2. ^{1}H NMR spectra recorded for (a) P(St-*co*-NBDAE-*co*-SPMA)$_{20}$ and (b) P(St-*co*-NBDAE-*co*-SPMA)$_{20}$-*b*-P(NIPAM-*co*-RhBAM)$_{60}$ in $CDCl_3$.

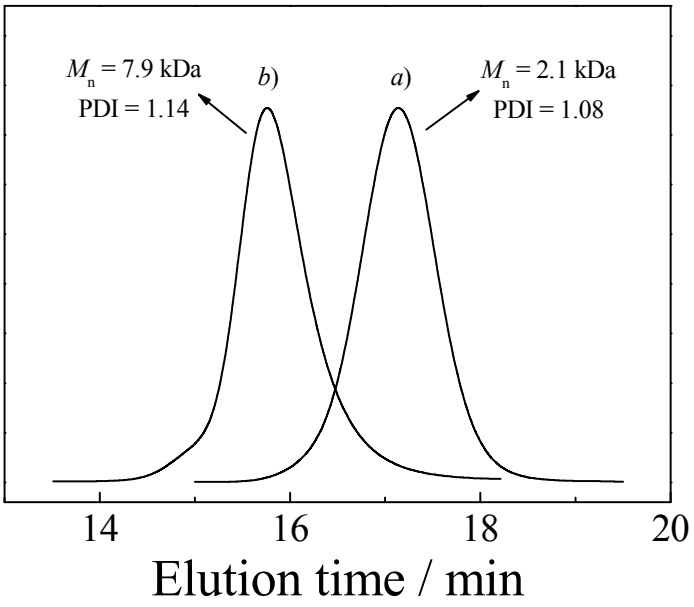

Figure S3. THF GPC traces recorded for (a) P(St-*co*-NBDAE-*co*-SPMA)$_{20}$ and (b) P(St-*co*-NBDAE-*co*-SPMA)$_{20}$-*b*-P(NIPAM-*co*-RhBAM)$_{60}$.

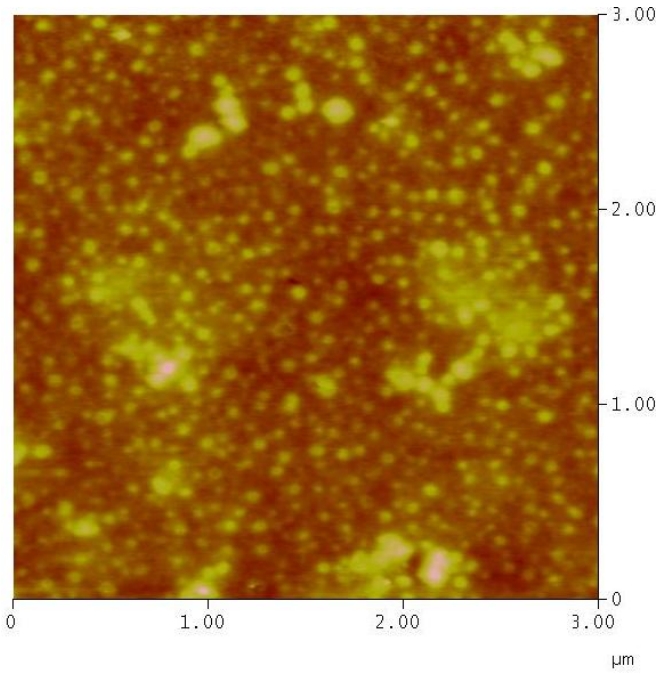

Figure S4. Typical AFM height image obtained by dip coating 0.05 g/L micellar solution of P(St-*co*-NBDAE-*co*-SPMA)$_{20}$-*b*-P(NIPAM-*co*-RhBAM)$_{60}$ onto mica at 25 ^{o}C. Z range is 15 nm.

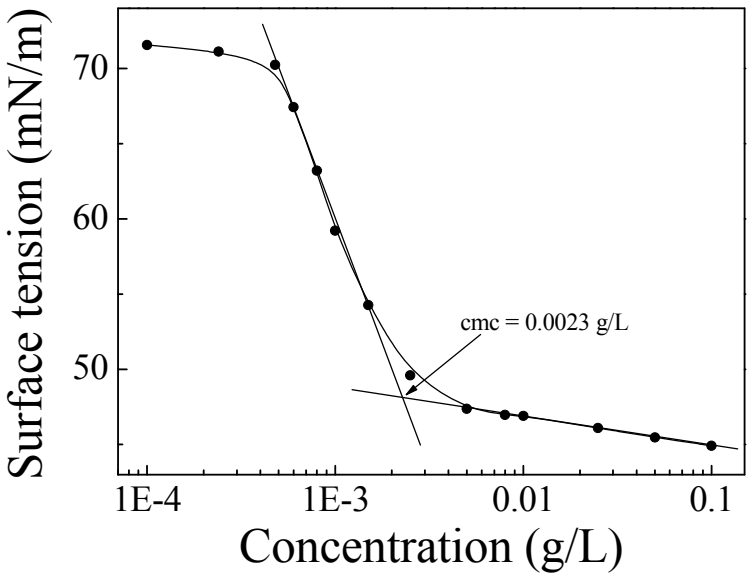

Figure S5. Determination of critical micellization concentration (cmc) from the experimental surface tension (γ) versus logarithm concentrations of P(St-*co*-NBDAE-*co*-SPMA)$_{20}$-*b*-P(NIPAM-*co*-RhBAM)$_{60}$ at 25 ^{o}C.

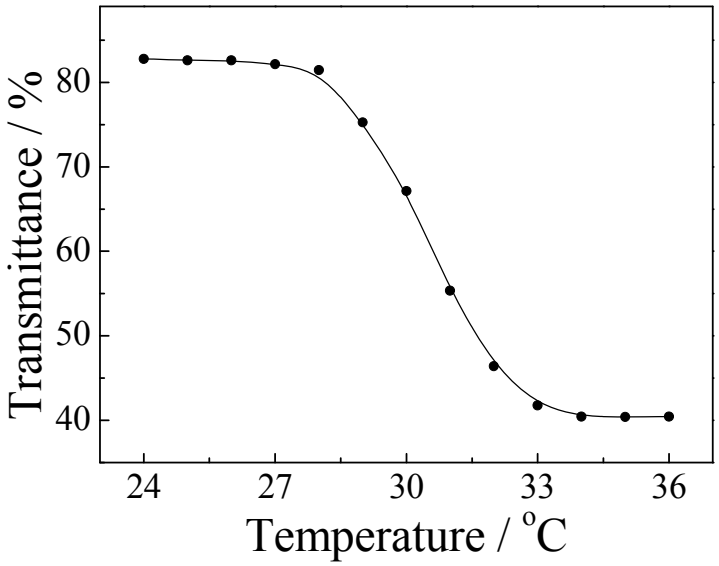

Figure S6. Temperature dependence of optical transmittance at 800 nm obtained for 1.0 g/L aqueous solution of P(St-*co*-NBDAE-*co*-SPMA)$_{20}$-*b*-P(NIPAM-*co*-RhBAM)$_{60}$.

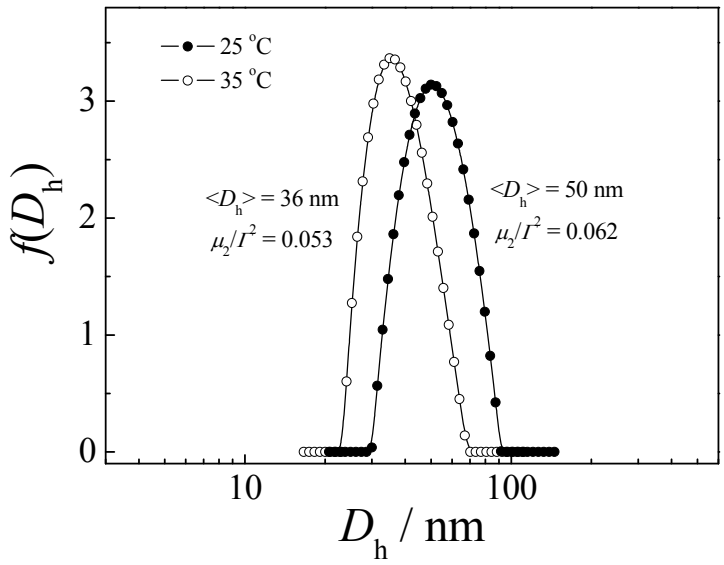

Figure S7. Hydrodynamic diameter distributions, $f(D_h)$, obtained for 0.05 g/L micellar solution of P(St-*co*-NBDAE-*co*-SPMA)$_{20}$-*b*-P(NIPAM-*co*-RhBAM)$_{60}$ diblock copolymer at 25 ^{o}C and 35 ^{o}C, respectively.

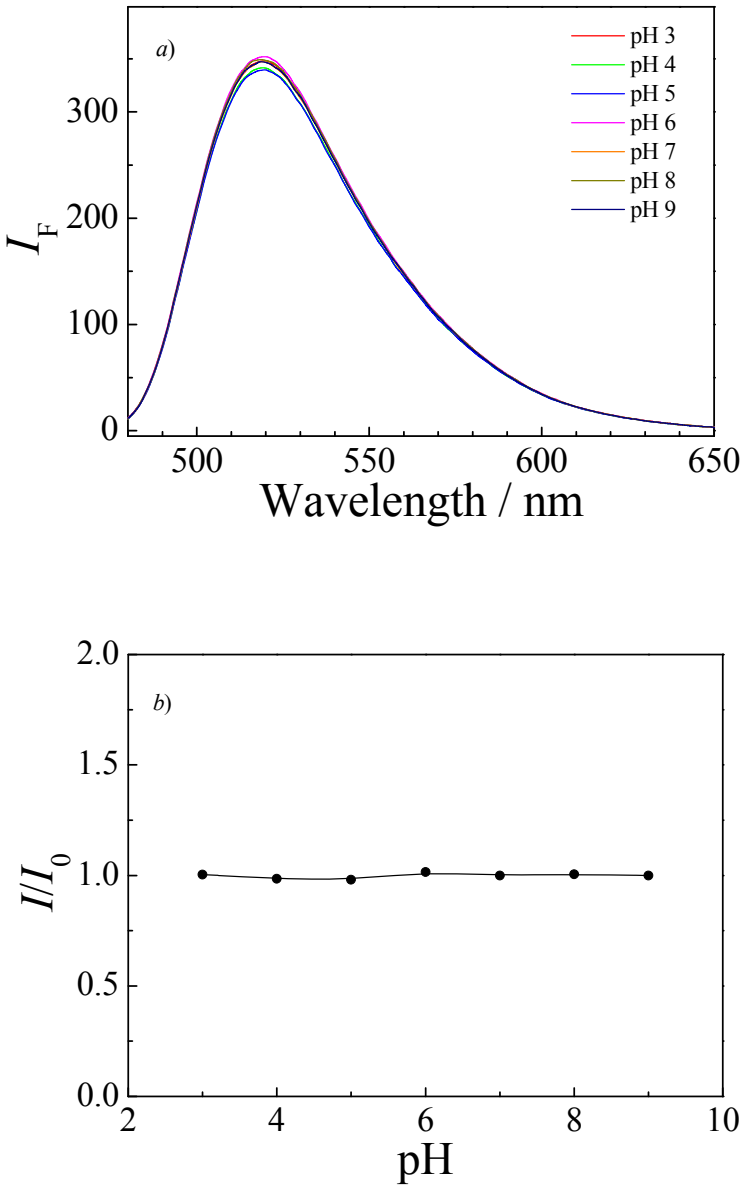

Figure S8. (a) Fluorescence emission spectra and (b) fluorescence intensity changes (λ_{ex} = 470 nm, λ_{em} = 518 nm; slit widths: Ex. 5 nm, Em. 5 nm) recorded for 0.05 g/L micellar solution of P(St-*co*-NBDAE)$_{20}$-*b*-PNIPAM$_{61}$ (25 ^{o}C) in the range of pH 3-9.

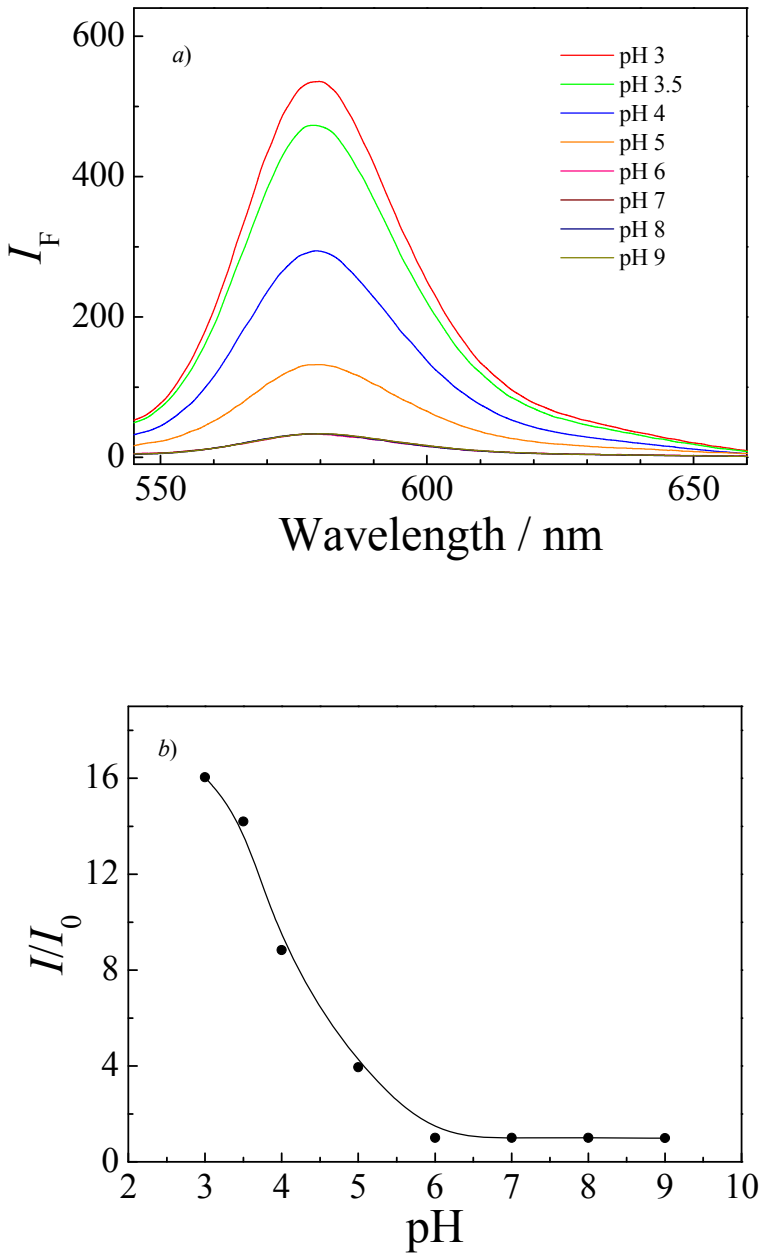

Figure S9. (a) Fluorescence emission spectra and (b) fluorescence intensity changes (λ_{ex} = 500 nm, λ_{em} = 580 nm; slit widths: Ex. 5 nm, Em. 5 nm) recorded for 0.05 g/L micellar solution of PS_{21}-*b*-P(NIPAM-*co*-RhBAM)$_{60}$ (25 ^{o}C) in the range of pH 3-9.

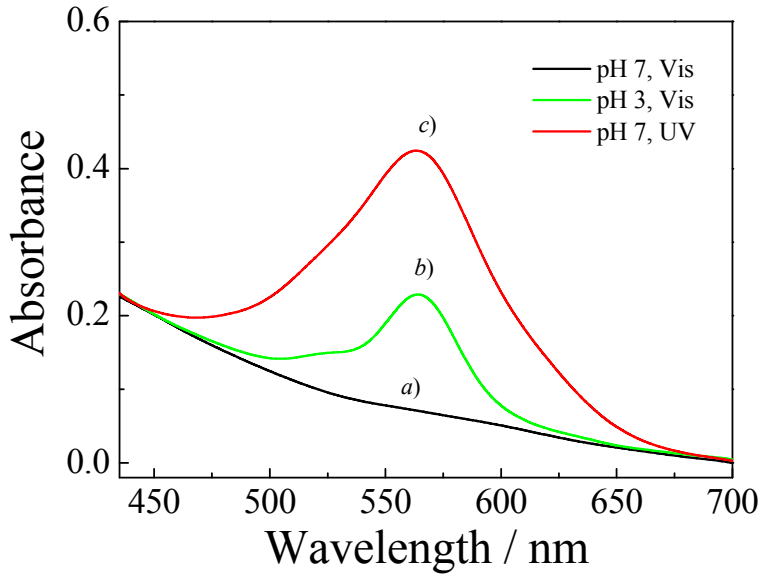

Figure S10. Absorption spectra recorded for 0.05 g/L micellar solution (25 ^{o}C) of P(St-*co*-NBDAE-*co*-SPMA)$_{20}$-*b*-P(NIPAM-*co*-RhBAM)$_{60}$ at varying conditions: (a) pH 7 upon visible light irradiation for 10 min; (b) pH 3 upon visible light irradiation for 10 min; (c) pH 7 upon UV irradiation (365 nm) for 2 min.

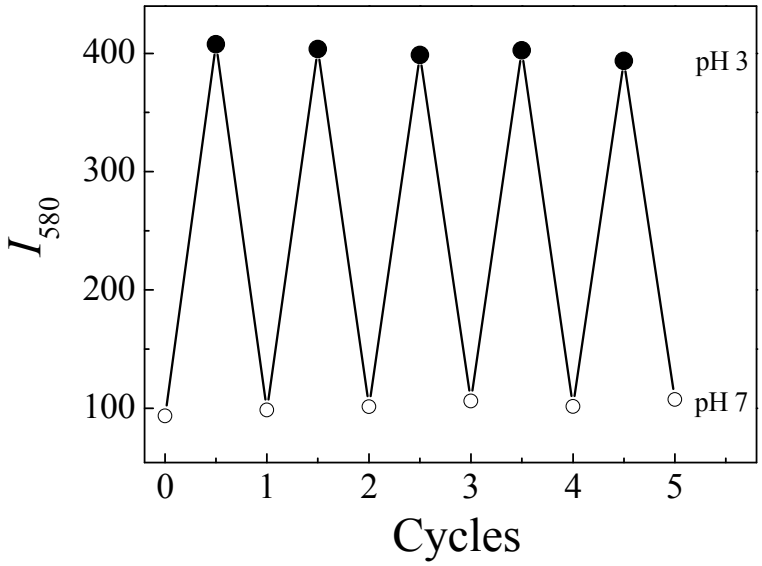

Figure S11. Fluorescence intensity changes (λ_{ex} = 470 nm, λ_{em} = 580 nm; slit widths: Ex. 5 nm, Em. 5 nm) of the micellar solution upon cycles between pH 3 and pH 7.

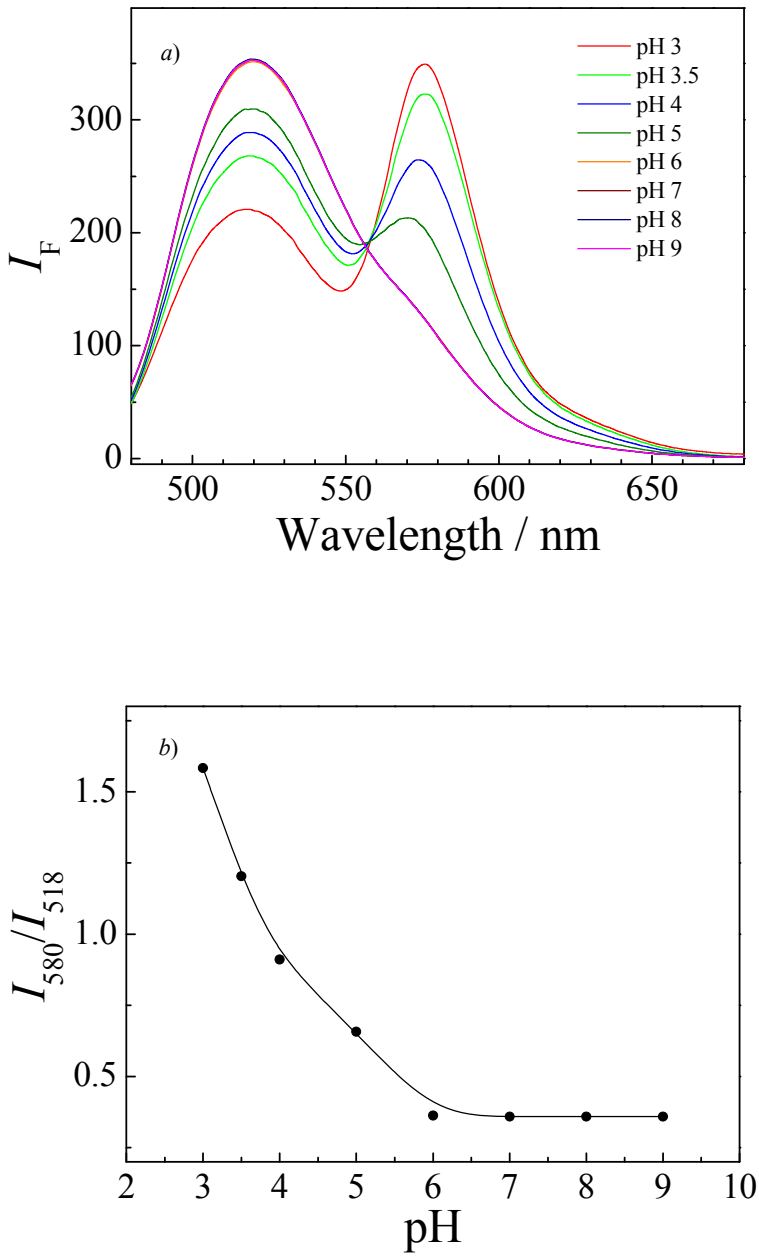

Figure S12. (a) Fluorescence emission spectra and (b) fluorescence intensity ratio changes (I_{580}/I_{518}; λ_{ex} = 470 nm, slit widths: Ex. 5 nm, Em. 5 nm) recorded for 0.05 g/L micellar solution of P(St-*co*-NBDAE)$_{20}$-*b*-P(NIPAM-*co*-RhBAM)$_{60}$ (25 ^{o}C) in the range of pH 3-9.

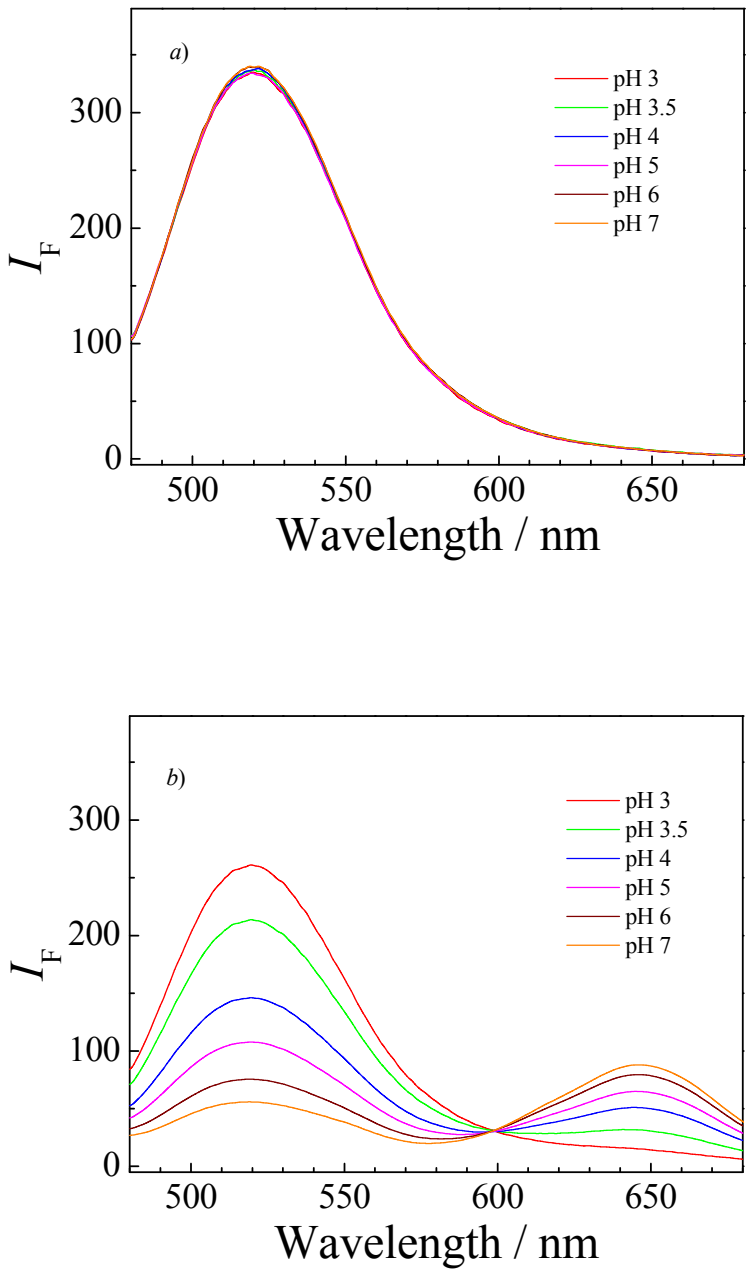

Figure S13. Fluorescence emission spectra (λ_{ex} = 470 nm, slit widths: Ex. 5 nm, Em. 5 nm) recorded for 0.05 g/L micellar solution of P(St-*co*-NBDAE-*co*-SPMA)$_{20}$-*b*-PNIPAM$_{60}$ (25 ^{o}C) in the range of pH 3-7 after irradiation with (a) visible light (10 min) and (b) UV light (365 nm, 2 min), respectively.

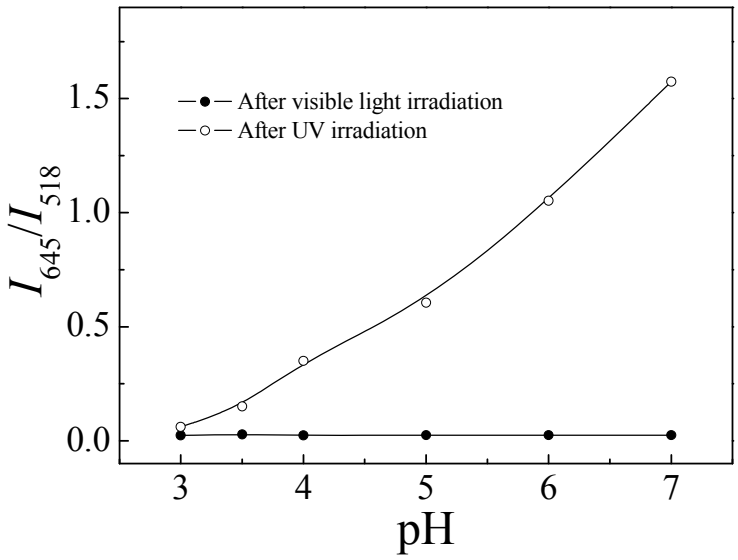

Figure S14. Fluorescence intensity ratio changes (I_{645}/I_{518}; λ_{ex} = 470 nm, slit widths: Ex. 5 nm, Em. 5 nm) recorded for 0.05 g/L aqueous solution of P(St-*co*-NBDAE-*co*-SPMA)$_{20}$-*b*-PNIPAM$_{60}$ (25 ^{o}C) in the range of pH 3-7 after irradiation with (●) visible light (10 min) and (○) UV light (365 nm, 2 min), respectively.

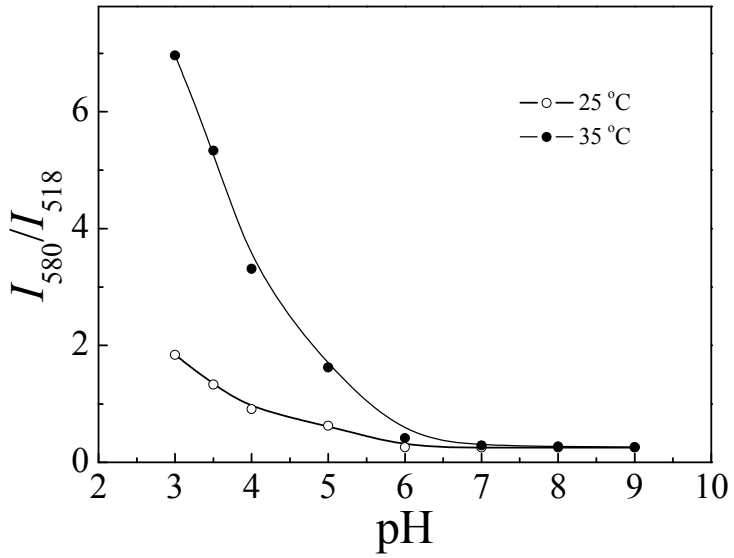

Figure S15. pH-dependent fluorescence intensity ratio changes (I_{580}/I_{518}; λ_{ex} = 470 nm, slit widths: Ex. 5 nm, Em. 5 nm) recorded for 0.05 g/L aqueous solution of P(St-*co*-NBDAE-*co*-SPMA)$_{20}$-*b*-P(NIPAM-*co*-RhBAM)$_{60}$ (after visible light irradiation for 10 min) at (○) 25 °C and (●) 35 °C, respectively.

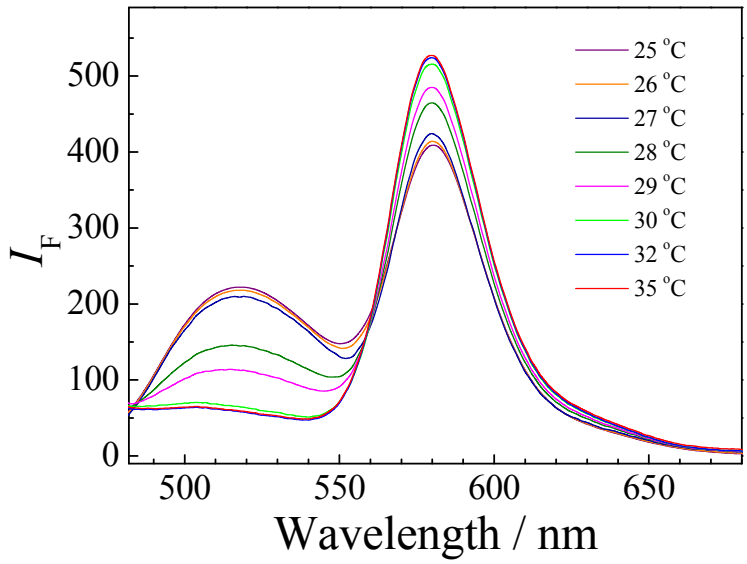

Figure S16. Fluorescence emission spectra (λ_{ex} = 470 nm, slit widths: Ex. 5 nm, Em. 5 nm) recorded for 0.05 g/L aqueous solution (pH 3, after visible light irradiation for 10 min) of P(St-*co*-NBDAE-*co*-SPMA)$_{20}$-*b*-P(NIPAM-*co*-RhBAM)$_{60}$ in the temperature range of 25-35 ^{o}C.

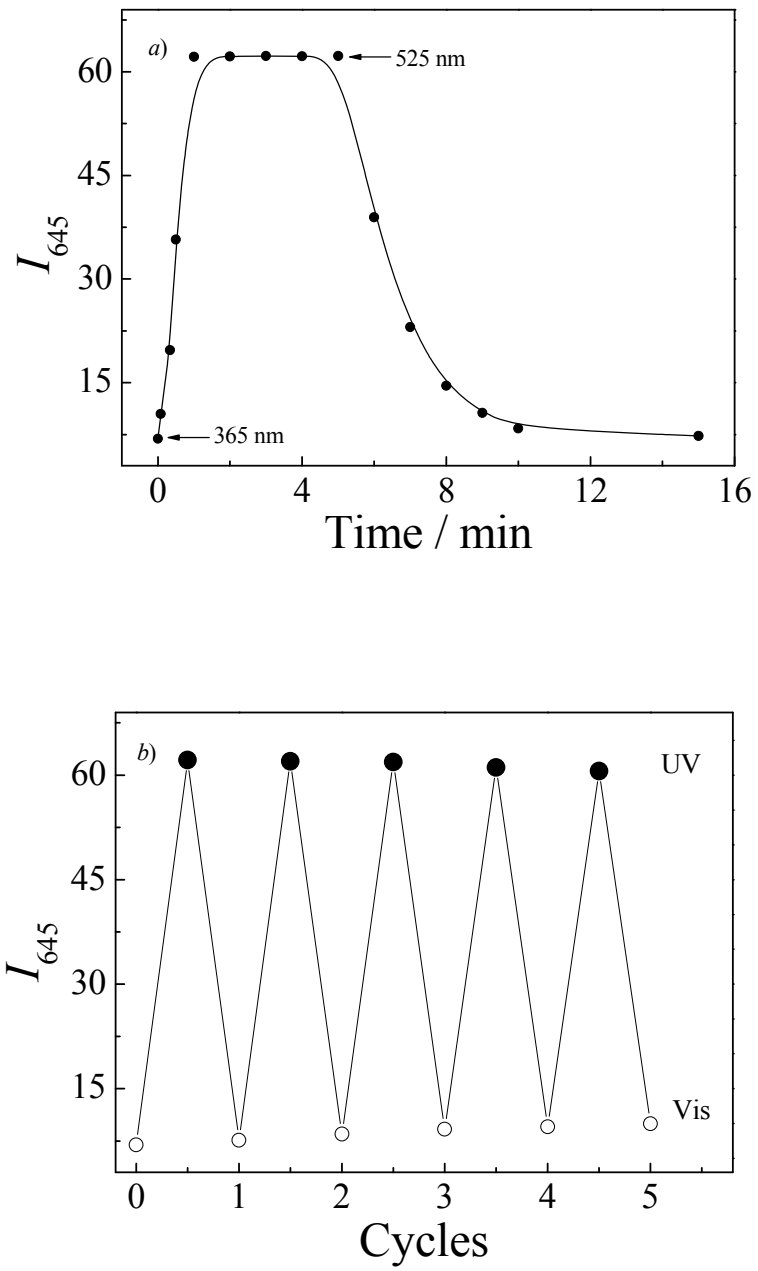

Figure S17. (a) Fluorescence response (λ_{ex} = 470 nm, λ_{em} = 645 nm; slit widths: Ex. 5 nm, Em. 5 nm) recorded for 0.05 g/L aqueous solution of P(St-*co*-NBDAE-*co*-SPMA)$_{20}$-*b*-P(NIPAM-*co*-RhBAM)$_{60}$ at 25 ^{o}C and pH 7 upon irradiation with UV light (365 nm) for 5 min and then with visible light (525 nm). (b) Fluorescent intensity changes of the micellar solution upon repeated cycles of UV irradiation (365 nm, duration of 2 min) and visible light irradiation (525 nm, 10 min).

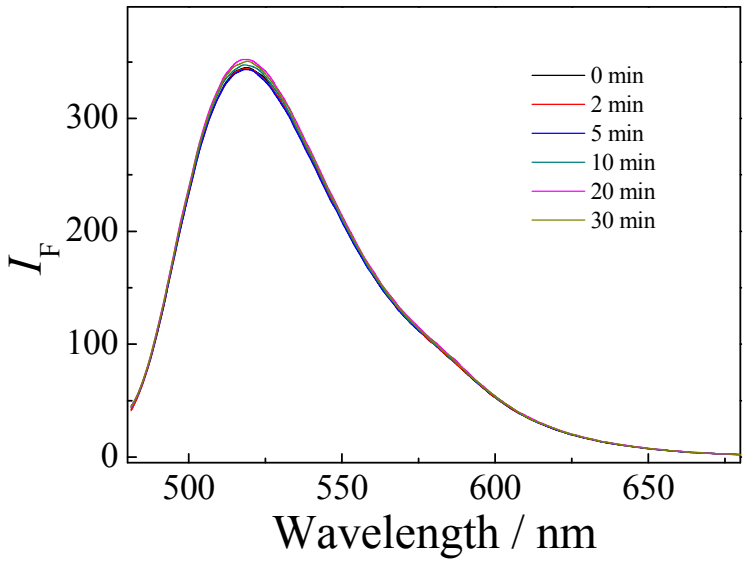

Figure S18. Time evolution of fluorescence spectra (λ_{ex} = 470 nm, slit widths: Ex. 5 nm, Em. 5 nm) recorded for 0.05 g/L aqueous solution (25 ^{o}C and pH 7) of P(St-*co*-NBDAE)$_{20}$-*b*-P(NIPAM-*co*-RhBAM)$_{60}$ upon UV (365 nm) irradiation.